



# INITIAL FIRE SUPPRESSION REACTIONS OF HALONS PHASE III-MOLECULAR BEAM EXPERIMENTS INVOLVING HALON CLUSTERS

E.A. WALTERS, J.R. GROVER, R.E. TAPSCOTT,  
J.T. CLAY, JR., D.L. ARNEBERG, M.H. WALL,  
J.S. NIMITZ, AND H.D. BEESON

NEW MEXICO ENGINEERING RESEARCH  
INSTITUTE  
UNIVERSITY OF NEW MEXICO  
ALBUQUERQUE NM 87131

SEPTEMBER 1990

FINAL REPORT

JUNE 1988 — APRIL 1989

DTIC  
ELECTE  
NOV 13 1991  
S D C

91-15377



APPROVED FOR PUBLIC RELEASE: DISTRIBUTION UNLIMITED



**ENGINEERING RESEARCH DIVISION**  
Air Force Engineering & Services Center  
ENGINEERING & SERVICES LABORATORY  
Tyndall Air Force Base, Florida 32403



91 1113 002

NOTICE

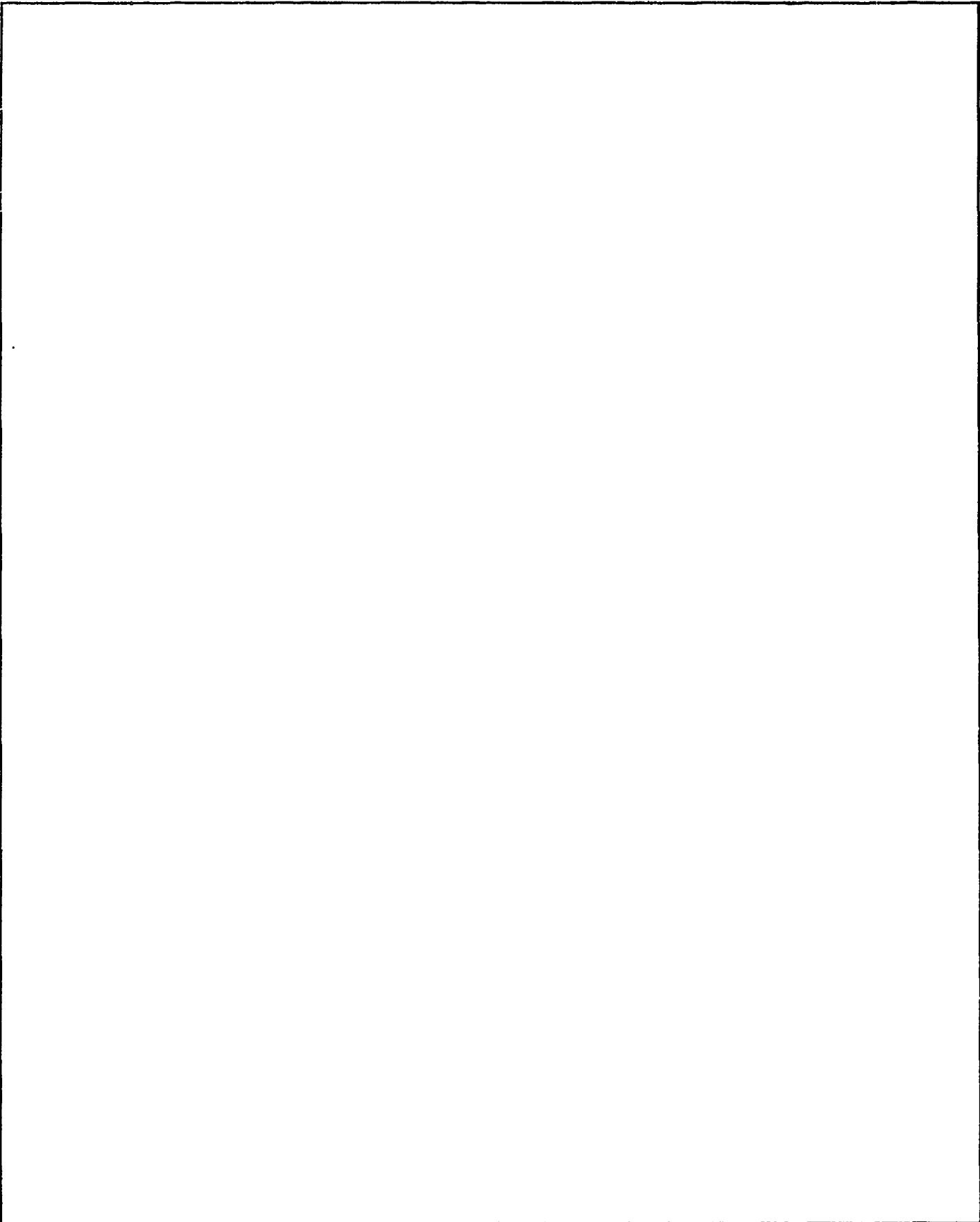
PLEASE DO NOT REQUEST COPIES OF THIS REPORT FROM  
HQ AFESC/RD (ENGINEERING AND SERVICES LABORATORY).  
ADDITIONAL COPIES MAY BE PURCHASED FROM:

NATIONAL TECHNICAL INFORMATION SERVICE  
5285 PORT ROYAL ROAD  
SPRINGFIELD, VIRGINIA 22161

FEDERAL GOVERNMENT AGENCIES AND THEIR CONTRACTORS  
REGISTERED WITH DEFENSE TECHNICAL INFORMATION CENTER  
SHOULD DIRECT REQUESTS FOR COPIES OF THIS REPORT TO:

DEFENSE TECHNICAL INFORMATION CENTER  
CAMERON STATION  
ALEXANDRIA, VIRGINIA 22314

REPORT DOCUMENTATION PAGE			Form Approved OMB No. 0704-0188	
Public reporting burden for this collection of information is estimated to average 1 hour per response, including the time for reviewing instructions, searching existing data sources, gathering and maintaining the data needed, and completing and reviewing the collection of information. Send comments regarding this burden estimate or any other aspect of this collection of information, including suggestions for reducing this burden, to Washington Headquarters Services, Directorate for Information Operations and Reports, 1215 Jefferson Davis Highway, Suite 1204, Arlington, VA 22202-4302, and to the Office of Management and Budget, Paperwork Reduction Project (0704-0188), Washington, DC 20503.				
1. AGENCY USE ONLY (Leave blank)		2. REPORT DATE September 1990		3. REPORT TYPE AND DATES COVERED Final Report June 1988 - April 1989
4. TITLE AND SUBTITLE  INITIAL FIRE SUPPRESSION REACTIONS OF HALONS PHASE III -- MOLECULAR BEAM EXPERIMENTS INVOLVING HALON CLUSTERS			5. FUNDING NUMBERS  F29601-C-87-0001	
6. AUTHOR(S) EDWARD A. WALTERS, J. ROBB GROVER, ROBERT E. TAPSCOTT, JAMES T. CLAY, JR., DAVID L. ARNEBERG, MARK H. WALL, JONATHAN S. NIMITZ, AND HAROLD D. BEESON				
7. PERFORMING ORGANIZATION NAME(S) AND ADDRESS(ES)  New Mexico Engineering Research Institute University of New Mexico Albuquerque, New Mexico 87131			8. PERFORMING ORGANIZATION REPORT NUMBER  SS 2.10(1)	
9. SPONSORING/MONITORING AGENCY NAME(S) AND ADDRESS(ES)  Engineering and Services Laboratory Air Force Engineering and Services Center Tyndall Air Force Base, Florida 32403			10. SPONSORING/MONITORING AGENCY REPORT NUMBER  ESL-TR-89-50	
11. SUPPLEMENTARY NOTES  Availability of this report is specified on reverse of front cover.				
12a. DISTRIBUTION/AVAILABILITY STATEMENT  Approved for public release; distribution is unlimited.			12b. DISTRIBUTION CODE	
13. ABSTRACT (Maximum 200 words)  The system of Halon 1301 (CF <sub>3</sub> Br) and molecular oxygen (O <sub>2</sub> ) was carefully studied. Small, isolated molecular clusters of Halon 1301 and the oxygen-atom, flame free radical precursor O <sub>2</sub> were formed in a supersonic molecular beam, and chemical reactions were initiated within the clusters by dissociative photoionization. The fragments formed were identified by mass spectrometry, and the ionization and appearance potentials for many of the species in this binary system were determined. The most striking result is the inability to detect oxygenated fragments of dissociative photoionization of the complex CF <sub>3</sub> Br•O <sub>2</sub> . The results hold important mechanistic implications for the role of CF <sub>3</sub> Br in fire extinguishment and in guiding the search for alternative firefighting agents.				
14. SUBJECT TERMS  Halon 1301, Oxygen, Clusters, Molecular beam, Dissociative photoionization, Flame suppression			15. NUMBER OF PAGES	
			16. PRICE CODE	
17. SECURITY CLASSIFICATION OF REPORT  UNCLASSIFIED	18. SECURITY CLASSIFICATION OF THIS PAGE  Unclassified	19. SECURITY CLASSIFICATION OF ABSTRACT  Unclassified	20. LIMITATION OF ABSTRACT  Unclassified	



## EXECUTIVE SUMMARY

### A. OBJECTIVE

The overall objective of this effort is to provide information on the detailed mechanism of fire extinguishment by halons to guide the search for alternative firefighting agents. The purpose of this Phase III study was to prepare and characterize a small, isolated cluster of Halon 1301 ( $\text{CF}_3\text{Br}$ ) and the oxygen-atom flame free radical precursor  $\text{O}_2$  in a supersonic molecular beam, and to initiate reaction within the cluster by dissociative photoionization. Examination of the fragments obtained provides insight into the mechanism of halon action.

### B. BACKGROUND

In Phase II of this project, an experimental approach to the study of the initial fire suppression reactions of halons was verified and preliminary experiments were conducted. Three experimental methods were examined: laser Raman spectroscopy, isolation of products on an argon matrix followed by Fourier transform infrared spectroscopy, and photoionization of molecular clusters followed by mass spectrometry. It was determined that photoionization mass spectrometry was the most effective technique for studying the initial reaction of halons with free radicals.

### C. SCOPE

In this phase of the project one system of a halon molecule (Halon 1301,  $\text{CF}_3\text{Br}$ ) and a flame free radical precursor ( $\text{O}_2$ ) was carefully studied. Thermodynamic properties of the clusters and fragments were measured.



Approved by	
Special Agent	
Date	
Justification	
By	
Distribution/	
Availability Codes	
Dist	Avail and/or Special
A-1	

#### D. METHODOLOGY

Two separate pieces of equipment were used. One was the molecular beam apparatus at the University of New Mexico and the other was the Brookhaven National Laboratory molecular beam apparatus used in conjunction with the vacuum ultraviolet synchrotron ring at the National Synchrotron Light Source.

#### E. TEST DESCRIPTION

In both apparatuses, samples from a supersonic molecular beam of clusters of Halon 1301 and  $O_2$  molecules were passed through a photon ionization source, then into a mass spectrometer. Molecules and ions resulting from the reactions of  $CF_3Br$  and  $O_2$  were identified by their characteristic mass spectral patterns.

#### F. RESULTS

The thermodynamic properties of several halon fragments were measured. One striking result is that no oxygenated fragments of the halon molecule were observed.

#### G. CONCLUSIONS

The lack of oxygenated halon fragments supports the theory that halons do not extinguish flames by trapping oxygen radicals. The extremely weak bond in  $CF_3Br^+$  suggests that Br atoms enter the flames via the ion  $CF_3Br^+$  and not from  $CF_3Br$  itself. Some evidence indicates that the  $CF_3$  portion of the halon molecule may have a more significant role in flame extinguishment than previously suspected.

## H. RECOMMENDATIONS

Future work should direct attention to the two other members of the triad of flame free radicals, H and OH. Therefore, it is recommended that the dissociative photoionization approach to weakly bound clusters of Halon 1301 and flame free radical precursors be extended to H and OH precursors. The results of these studies are expected to provide a good picture of the chemistry of the halon-flame interaction and to give a solid basis for suggesting alternative agents.

## PREFACE

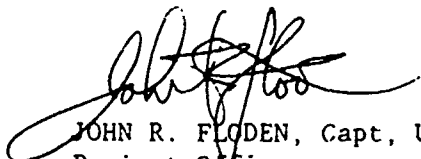
This report was prepared by the New Mexico Engineering Research Institute (NMERI), University of New Mexico, Albuquerque, New Mexico 87131, under contract F29601-87-C-0001, for the Engineering and Services Laboratory, Air Force Engineering and Services Center, Tyndall Air Force Base, Florida 32403.

This report summarizes work done between January 1988 and July 1989. The HQ AFESC/RDCF Project Officers were Major E. Thomas Morehouse and Capt John R. Floden.


Mr. Joseph L. Walker, Chief, Fire Technology Branch, Air Force Engineering and Services Laboratory, provided invaluable information and discussions for successful completion of the project. Dr. Robert E. Tapscott, New Mexico Engineering Research Institute, University of New Mexico, participated in establishing the research direction and served as the liaison with the Air Force sponsors.

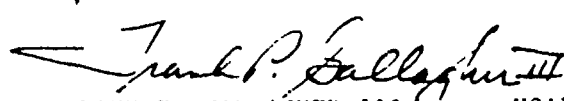
This report has been reviewed by the Public Affairs Officer (PA) and is releasable to the National Technical Information Service (NTIS). At NTIS it will be available to the general public, including foreign nationals.

This technical report has been reviewed and is approved for publication.

  
JOHN R. FLODEN, Capt, USAF  
Project Officer

  
WILLIAM S. STRICKLAND  
Chief, Engineering Research Division

  
JOSEPH L. WALKER  
Chief, Air Base Fire Protection  
and Crash Rescue Systems Branch

  
FRANK P. GALLAGHER III, Col, USAF  
Director, Engineering and Services  
Laboratory

## TABLE OF CONTENTS

Section	Title	Page
I	INTRODUCTION.....	1
	A. OBJECTIVE.....	1
	B. BACKGROUND.....	1
	C. SCOPE.....	1
	D. TECHNICAL APPROACH.....	2
II	EXPERIMENTAL.....	4
	A. THE UNM APPARATUS.....	4
	B. THE BROOKHAVEN APPARATUS.....	8
	C. BEAM ANALYSIS.....	10
III	RESULTS.....	21
IV	CONCLUSIONS.....	33
V	RECOMMENDATIONS FOR FUTURE WORK.....	34
	REFERENCES.....	35

# LIST OF FIGURES

Figure	Title	Page
1	Nozzle Beam Sampling and Ion Source.....	5
2	Schematic Diagram of Photoionization Mass Spectrometer.....	6
3	Mass Spectrum of $\text{CF}_3\text{Br}$ .....	23
4	Mass Spectrum of a 1:20 Mixture of $\text{CF}_3\text{Br}$ in $\text{O}_2$ .....	24
5	$\text{CF}_3\text{Br}^+$ Wavescan.....	26
6	$\text{CF}_3\text{BrO}_2^+$ Wavescan, 1035-1110 Å.....	27
7	$\text{CF}_3\text{BrO}_2^+$ Wavescan, 1070-1110 Å.....	28
8	$\text{CF}_3^+$ Wavescan.....	29
9	Energy Diagram for Neutral and Ionic Species in the $\text{CF}_3\text{Br}$ System.....	31
10	More Detailed Mass Spectra of 1:20 $\text{CF}_3\text{Br}:\text{O}_2$ .....	32

# LIST OF TABLES

Table	Title	Page
1	DISSOCIATION ENERGIES OF THE WEAK MOLECULAR COMPLEXES $\text{C}_6\text{H}_6 \cdot \text{O}_2$ , $\text{C}_6\text{F}_6 \cdot \text{O}_2$ , $\text{CF}_3\text{Br} \cdot \text{O}_2$ , AND THEIR IONS.....	22

## LIST OF SYMBOLS

d	The number density (intensity) of the neutral dimer.
D	The number density (intensity) of the dimer ion.
$D(A \cdot A)$	The binding energy of the dimer of two molecules of A. Similar terms refer to $A \cdot B$ , $A_2 \cdot A_1$ , and $A_2 \cdot B$ .
f	Detection efficiency: The probability that a particular species is detected by the mass spectrometer. May have the subscript m, d, or t, representing the monomer, dimer, or trimer, respectively.
I	Intensity of photon (or electron) crossing beam.
$\ell$	Effective path length of the photons or electrons through the molecular beam.
M	The number density of the monomer ion that arises from dimers, trimers, and higher order clusters.
t	The number density (intensity) of the neutral trimer.
T	The number density (intensity) of the trimer ion.
$\alpha$	Probability that ionization of the dimer produces the monomer ion.
$\beta$	Probability that ionization of the trimer produces the dimer ion.
$\delta$	Probability that ionization of the dimer produces the dimer ion.

LIST OF SYMBOLS  
(CONTINUED)

- $\epsilon$  Probability that ionization of the trimer produces the monomer ion.
- $\eta$  Probability that ionization of the trimer produces the trimer ion.
- $\rho$  Beam number density; may have the subscript d or t, referring to the dimer or trimer, respectively.
- $\sigma$  Total ionization cross section; may have the subscript d or t, referring to the dimer or trimer, respectively.

## SECTION I

### INTRODUCTION

#### A. OBJECTIVE

The purpose of this study was to prepare and characterize a small, isolated cluster of Halon 1301 ( $\text{CF}_3\text{Br}$ ) and the O-atom flame free radical precursor,  $\text{O}_2$ , in a supersonic molecular beam, and to initiate a chemical reaction within the cluster by dissociative photoionization. The critical question was whether oxygenated fragments of  $\text{CF}_3\text{Br}$  could be found and, if so, what their thermodynamic (stability) parameters would be. The results of this experiment provide information on the detailed mechanism of fire extinguishment by  $\text{CF}_3\text{Br}$  and consequently are important in guiding the search for alternative agents.

#### B. BACKGROUND

In Phase II of this project, an experimental approach to the study of the initial fire suppression reactions of halons was verified and preliminary experiments were conducted. The verification consisted of laboratory evaluations of laser Raman spectroscopy, matrix isolation Fourier transform infrared spectroscopy (FTIR), and photoionization mass spectrometry. These experiments led to the conclusion that photoionization mass spectrometry combines the requisite analytical sensitivity with versatility for determining the critical features of initial halon interactions with flames. It was decided that this is the most cost-effective and rapid technique for the continued studies of reactions between free radicals and halons.

#### C. SCOPE

In this phase of the project one system of a halon molecule and a flame free radical precursor was carefully studied. On the basis of the bulb experiments described in Phase II and the exceptional observation that no

oxygenated products were found on photolysis of mixtures of  $\text{CF}_2\text{BrCl}$  plus  $\text{O}_2$  or  $\text{NO}_2$ , it was judged wise to use a halon plus  $\text{O}_2$  sample for this study. Past experience of  $\text{O}_2$  complexes with  $\text{C}_6\text{H}_6$  and  $\text{C}_6\text{F}_6$  has shown that dissociative photoionization results in substantial production of the oxygenated fragment ions  $\text{C}_6\text{H}_6\text{O}^+$  and  $\text{C}_6\text{F}_6\text{O}^+$ . Even in the very weakly bound cluster  $\text{O}_2\cdot\text{Ar}$  it is possible to produce an oxygenated ion,  $\text{ArO}^+$ . If no oxygenated ions are formed on dissociative photoionization of halon plus  $\text{O}_2$  complexes, this result has important fire extinguishment mechanistic implications. As an experimental consideration, the halon  $\text{CF}_3\text{Br}$  (Halon 1301) was used with  $\text{O}_2$  to form the weakly bound complex to be studied. The result is a simpler mass spectrum, by virtue of fewer isotopes, than a halon containing two bromine atoms or a bromine and a chlorine atom.

#### D. TECHNICAL APPROACH

The experimental protocol followed for the Phase III study was:

1. Preparation of  $\text{CF}_3\text{Br}$  and  $\text{O}_2$  mixtures in various proportions in 4L stainless steel cylinders.
2. A study of the pressure dependence of the mass spectrum of these mixtures when expanded through a supersonic nozzle and ionized by 584 Å (21.22 eV) light from a He I discharge lamp using the UNM apparatus, and by 700 Å light at the National Synchrotron Light Source at Brookhaven National Laboratory.
3. Analysis of these data by solution of a set of simultaneous equations to give the conditions under which the heterodimer clusters,  $\text{CF}_3\text{Br}\cdot\text{O}_2$ , are predominant.
4. Design and construction of an ion kinetic energy analyzer for the quadrupole mass spectrometer.
5. A complete study of the optimized  $\text{CF}_3\text{Br} + \text{O}_2$  mixture by dissociative photoionization using the tunable vacuum ultraviolet

(VUV) light source, a 750 MeV synchrotron, at Brookhaven National Laboratory.

6. Analysis of the results and recommendations for future work.

## SECTION II

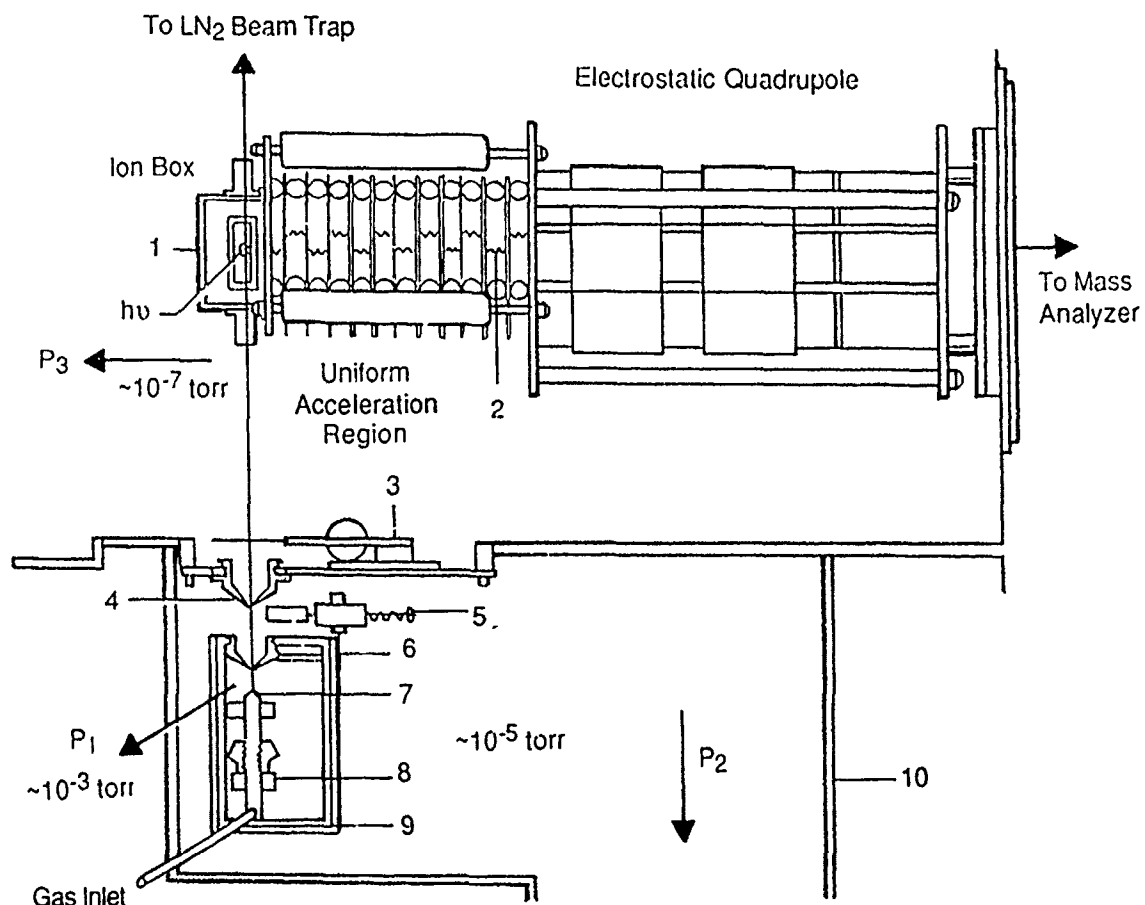
### EXPERIMENTAL

Two separate pieces of equipment were used. One was the molecular beam apparatus at the University of New Mexico and the other was the Brookhaven National Laboratory molecular beam apparatus used in conjunction with the VUV synchrotron ring at the National Synchrotron Light Source.

#### A. THE UNM APPARATUS

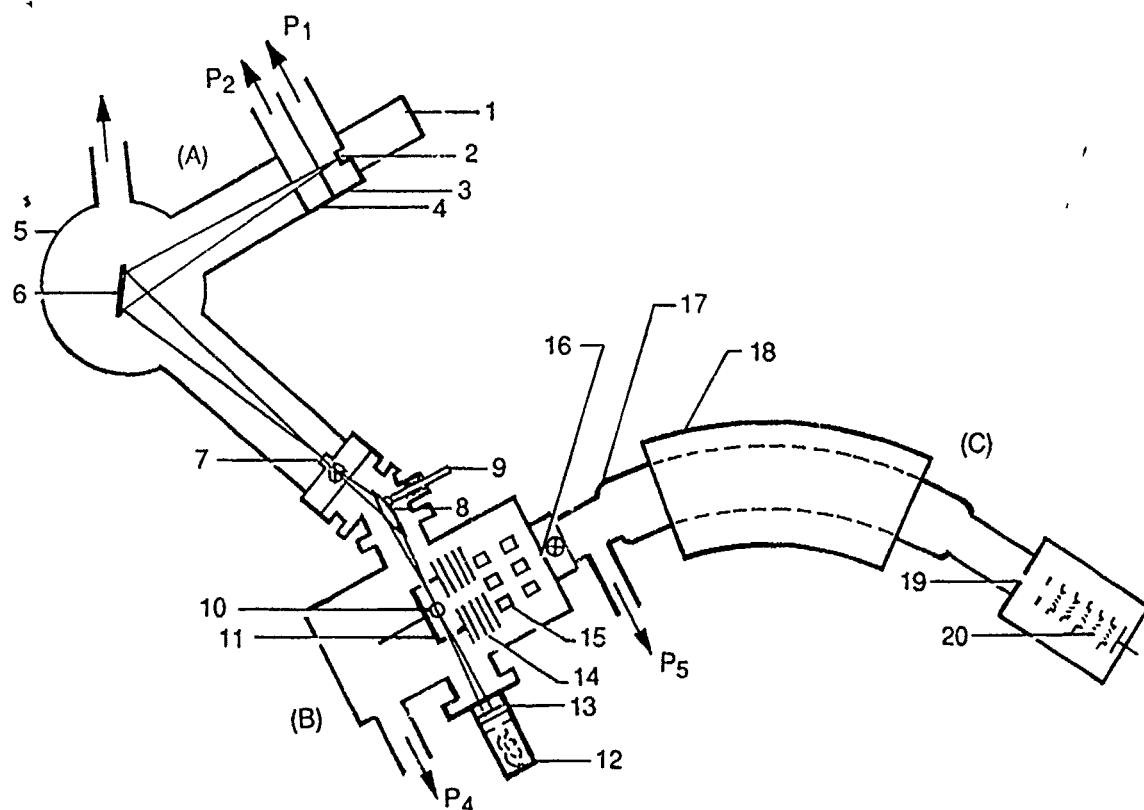
The apparatus used consists of a moderate resolution magnetic sector mass spectrometer that has been modified to include a supersonic molecular beam sampling system and a photon ionization source. Figures 1 and 2 illustrate the various elements in the experimental design.

A molecular beam is obtained by expanding a gas through a 0.004-inch diameter nozzle at stagnation pressures of up to 2000 torr. The nozzle exhaust chamber is pumped by two 4-inch ring jet booster pumps which maintain a vacuum of approximately  $10^{-3}$  torr. The high intensity central portion of the expansion is extracted with a 0.018-inch diameter conical skimmer into a second differential pumping region. This chamber is pumped by a 4-inch diffusion pump to a pressure of less than  $10^{-5}$  torr. The expansion is further collimated by a 0.040-inch conical skimmer before entering the ionization chamber. Provision is made to flag the beam. A liquid nitrogen-cooled surface is used to trap those molecules that escape ionization. The main chamber pressure is maintained at less than  $3 \times 10^{-7}$  torr when the beam is running. On the basis of electron impact measurements on several compounds, beam densities are estimated to be between  $1 \times 10^{12}$  and  $3 \times 10^{12}$  molecules/cc in the ionization region.



(1) ion box at +10 kV (see text), (2)  $12 \times 10 \text{ M}\Omega$  to provide uniform acceleration of ions over 10 kV, (3) tuning fork chopper, (4) secondary skimmer, (5) electromagnetic beam flag, (6) primary skimmer and skimmer support, (7) nozzle, (8) nozzle support and bevel gears for nozzle advance, (9) nozzle exhaust chamber, (10) second differential pumping chamber; ( $P_1$ ) 575 liters/sec (see text), ( $P_2$ ) 700 liters/sec (see text) ( $P_3$ ) 1400 liters/sec 6" diffusion pump.

Figure 1. Nozzle Beam Sampling and Ion Source.



(A) light source-monochromator system, (B) ionization chamber, (C) mass analyzer and detector; (1) McPherson Model 630 D.C. capillary discharge lamp, (2) monochromator entrance slit, (3) first differential pumping chamber, (4) second differential pumping chamber, (5) 1/2-meter Seya-Namioka vacuum ultraviolet monochromator, (6) grating, (7) monochromator exit slit, (8) grazing incidence alignment mirror, (9) micrometer for mirror adjustment, (10) molecular beam crosses photon beam at right angles, (11) ion box, (12) photomultiplier tube, (13) sodium salicylate coated window, (14) uniform acceleration region, (15) electrostatic quadrupole, (16) mass spectrometer entrance slit, (17) drift tube, (18) 60°-sector electromagnet, (19) mass spectrometer exit slit, (20) electron multiplier; (P<sub>1</sub>) 47 liters/sec Roots blower, (P<sub>2</sub>) 700 liters/sec 4" diffusion pump, (P<sub>4</sub>) 700 liters/sec 6" diffusion pump, (P<sub>5</sub>) 700 liters/sec 4" diffusion pump.

Figure 2. Schematic Diagram of Photoionization Mass Spectrometer.

In the present work, large (4L) stainless steel bottles of premixed  $\text{CF}_3\text{Br}$  and  $\text{O}_2$  were prepared in ratios of 0.5:99.5, 1:99, and 5:95 ( $\text{CF}_3\text{Br}:\text{O}_2$ ). The stagnation pressures varied between 100 and 1800 torr. Mass spectra were recorded by manually tuning the magnet to the appropriate field strength.

The He I line at 584 Å (21.2 ev. arising from the  $1\text{P}$  to  $1\text{S}$  electronic transition) produced by a McPherson Model 630 D.C. capillary discharge lamp was used as a photon source. A long, notched 3-mm bore capillary was used as a light pipe to direct the VUV photons to intersect the molecular beam. This allowed windowless operation, provided there was strong differential pumping at the notch. A homebuilt photodiode was used to monitor the intensity of the photodiode helium lamp. The output was measured by a picoammeter. Signals were typically one to two orders of magnitude higher than the dark current.

The ionizer consists of a gold-plated stainless steel box that contains entrance and exit ports for the ultra-violet light, a filament-collector arrangement to provide electron bombardment capability, and an inner surface to which a small repelling voltage (+0.20 V) may be applied. Extracted positive ions were uniformly accelerated by a +10 kV potential into a pair of quadrupole lenses (References 1 and 2), which focused the ions into a line image at the mass spectrometer entrance slit.

Mass analysis was accomplished by a  $60^\circ$ -sector electromagnet with a 17.750-inch radius of curvature. The drift tube entrance and exit slits were opened wide enough to maximize ion transmission while maintaining sufficient resolution to separate 1 amu in 300 cleanly. Conventional pulse counting techniques were used for ion detection. The pressure in the drift tube and detection chamber was maintained at less than  $2 \times 10^{-7}$  torr.

The photoionization efficiency was determined by the ratio of ion signal to photon signal as a function of wavelength. The lamp intensity

remained stable to  $\pm 2$  percent at each point. For the situation in which a monochromator was used, known hydrogen atom and molecule emission lines were used for wavelength calibration (References 3 and 4).

Background corrections were found to be quite small. With the molecular beam flagged, the ion counting background rate was about 0.02-0.1 count/sec. Thus, reproducible ion signals of about 0.05 count/sec were detectable. Since a holographically recorded diffraction grating was used, stray light levels were substantially reduced. Under high-resolution conditions, it was possible to reproduce the spectrum given by Samson (Reference 4) in substantial detail.

#### B. THE BROOKHAVEN APPARATUS

The Brookhaven experiments were conducted at the 750-MeV electron storage ring of the National Synchrotron Light Source at Brookhaven National Laboratory. The apparatus has already been described in (Reference 5); however, certain details pertinent to the present study are amplified here. The molecular beams containing clusters were produced by jet expansion of gas through a nozzle 0.01 cm (0.004 in.) in diameter. The nozzle chamber was evacuated by an  $6000 \text{ L s}^{-1}$  diffusion pump backed by a  $240 \text{ m}^3 \text{ h}^{-1}$  ( $67 \text{ L s}^{-1}$ ) Roots blower, backed in turn by a  $30 \text{ m}^3 \text{ h}^{-1}$  mechanical pump. At 1000 torr of nozzle pressure, the jet expansion would typically be pressures of approximately  $5 \times 10^{-4}$  torr. A 0.1 cm skimmer was used, the nozzle-skimmer distance of 0.5 to 1 cm with adjustment for maximum beam intensity. The post-skimmer collimator was 0.3 cm in diameter and was evacuated by a  $500 \text{ L s}^{-1}$  turbomolecular pump. Under the above conditions the pressure in this region is typically  $2 \times 10^{-5}$  torr. The molecular beam intersected the ionizing photons in an interaction chamber at a point 11 cm from the nozzle and in the optimal ion-extraction region of a lens system that focused the ions on the entrance aperture of a quadrupole mass spectrometer equipped with a channeltron detector operating in the ion-counting mode. The interaction chamber and beam dump were pumped by two turbomolecular pumps with a combined pumping speed of  $700 \text{ L s}^{-1}$  plus a 15 K helium refrigerator

trap into which the molecular beam was directed. Interaction chamber pressures were approximately  $2 \times 10^{-7}$  torr under the above conditions. Ionizing photons of wavelength 584 Å (21.2 eV) were employed almost exclusively for the studies described here, to allow direct comparison with work done off-line using the He I line produced by conventional laboratory lamps. This photon energy is high enough to ionize anything of interest for the present work and provide the high threshold fragment ions  $F^+$  required in the analysis. The gas mixtures supplied to the nozzle were accurately mixed off-line and stored in large stainless steel tanks at pressures low enough to avoid condensation. For mixtures of gas plus the vapor of a liquid, the gas was bubbled through several centimeters of the liquid from an immersed frit, keeping a constant head pressure maintained by a hand-operated needle valve and monitored by a capacitance manometer. The nozzle pressure itself could be accurately controlled electronically to  $\pm 1$  torr via a capacitance manometer and a servomotor drive valve system.

For calibration of the mass spectrometer plus detector system for the mass dependence of the detection efficiency, a 1:1 mixture of  $CO_2$  and  $SF_6$  was expanded at a nozzle pressure of only 100 torr to avoid fractionation and clustering effects, and the relative intensities of the ions  $CO_2^+$ ,  $SF_3^+$ , and  $SF_5^+$  were measured. These intensities were compared with the published cross sections (References 6 and 7) to provide relative efficiencies up to mass 127. Efficiencies between masses 25 and 43 were estimated via plausible extensions of the efficiency curves. Approximate efficiencies at masses 156 and 234 were obtained from benzene cluster ions.

First, evidence is presented for the two important phenomena exploited in the analytical method described above. These phenomena are (a) the tendency for dissociative ionization of clusters to make monomer parent ions with higher probability than monomer fragment ions and (b) the practicability of measuring the ratio of coefficients  $\delta/\alpha$ . Delta ( $\delta$ ) is the probability that ionization of the dimer produces the dimer ion, and  $\alpha$  is the probability that ionization of the dimer produces the monomer ion.

## BEAM ANALYSIS

The work described here has been published (Reference 8). The technique of synthesizing weakly bound dimers and larger clusters in jet expansions is in widespread use. This method is quite general and simple to implement (References 9 and 10), but normally results in an array of cluster sizes. Accurate analysis of the resulting cluster distributions is often a significant problem. If a high-energy electron impact or photoionization mass spectrometer is used for analysis, extensive fragmentation of the clusters into smaller cluster ions and the monomer ion almost always occurs (for recent discussions, see References 11-15), so that quantitative analysis by this means alone has not yet proven practicable. However, if one wishes to carry out observations on one particular neutral cluster (e.g., a dimer) it may be important to maximize the beam density of the desired cluster among the products emerging from the nozzle and minimize the densities of the neighboring or otherwise interfering clusters. It is unfortunate that a number of workers have already published results that should be remeasured or reinterpreted due to the difficulty in establishing exactly which species is being studied in a jet expansion.

It would be very convenient to be able to effect the necessary optimization with respect to a given cluster utilizing only a mass spectrometer because it is a familiar instrument that is usually available. Indeed, van Deursen and Reuss published a useful algorithm for estimation of the conditions for the preparation of dimer beams, essentially free of interference from trimers and larger clusters, which they obtained from the study of expansions of unmixed simple gases, viz.  $H_2$ , Ne,  $N_2$ , Ar, and  $CO_2$  (Reference 16). Their prescription, though convenient, is too limited for application to the problems in which we are most interested; it does not locate the nozzle pressure at which the dimer beam density is at its maximum, and it does not treat expansions of gas mixtures. Also, their method gives a generalized estimate, which is often not accurate enough for the study of specific systems. What follows in this section is a partial but useful solution to this vexing problem, specifically the optimization of

jet expansions of mixed gases for the investigation of weak dimers with minimization of interference by trimers and larger clusters, that we have developed in the course of a series of photoionization studies of weakly bound dimers (References 17-19).

The method is first described for the expansion of a pure gas, then generalized to mixtures.

It is assumed that the jet expansion of the polyatomic gas A produces the clusters  $A_2$ ,  $A_3$ ,  $A_4$ , and so on, according to well-established behavior. As the pressure of the expanding gas (the nozzle pressure) increases from low values, the density of  $A_2$  in the expansion products first rises and becomes the most prominent cluster, goes through a maximum, and then falls, while the density of  $A_3$  rises and becomes dominant. The  $A_3$  maximizes and then falls as the density of  $A_4$  rises in its turn, and so on. It is also assumed that the mass spectrometric analysis of these species in a molecular beam collimated from the expansion and crossed by an electron or photon beam is carried out at a fixed high electron or ionizing photon energy level to produce the ions  $A^+$ ,  $A_2^+$ ,  $A_3^+$ , and so on, plus various ion fragments. The goal of the analysis is only to obtain the nozzle pressure dependence of the beam densities of the neutral dimer, and of the neutral trimer around the maximum of the dimer. For this analysis the intensities of the ions  $A^+$ ,  $A_2^+$ , and  $A_3^+$  are to be measured, for a given nozzle and temperature, from low nozzle pressures up to the pressure at which the intensity of  $A_3^+$  maximizes, above which pressure neutral clusters larger than trimers are significant (for simplicity we ignore the ion fragments here, but discuss their role further on.)

Let  $[A^+]_c$  be the observed (uncorrected) intensity of monomer ions  $A^+$  produced only from the dissociative ionization of clusters (obtained from the total  $A^+$  intensity by subtraction of the  $A^+$  intensity due to only the ionization of monomer A), let  $[A_2^+]$  be the observed intensity of dimer ions  $A_2^+$ , and let  $[A_3^+]$  be the observed intensity of trimer ions  $A_3^+$ . The beam number densities of the neutral dimer,  $\rho_d$ , and trimer,  $\rho_t$ , are related to

the observed ion intensities via the following expressions, neglecting tetramers and larger clusters where  $i$  is the intensity of the photon

$$[A^+]_c = f_m \alpha \sigma_d \rho_d \ell I + f_m \beta \sigma_t \rho_t \ell I \quad (1)$$

$$[A_2^+] = f_d \delta \sigma_d \rho_d \ell I + f_d \epsilon \sigma_t \rho_t \ell I \quad (2)$$

$$[A_3^+] = f_t \eta \sigma_t \rho_t \ell I \quad (3)$$

(or electron) crossing beam, assumed to be smaller in diameter than the molecular beam;  $\ell$  is the effective path length of the photons or electrons through the molecular beam; the electrons or photons are assumed to be negligibly attenuated;  $\sigma_d$  and  $\sigma_t$  are the total ionization cross sections of the dimers and trimers, respectively;  $\alpha$  is the probability that the ionization of the dimer produces the monomer ion;  $\beta$  is the probability that the ionization of the trimer produces the monomer ion;  $\delta$  and  $\epsilon$  are the probabilities that the dimer ion is produced by ionization of dimer and trimer, respectively;  $\eta$  is the probability that the ionization of the trimer produces the trimer ion; and  $f_m$ ,  $f_d$ , and  $f_t$  are the respective probabilities that the mass spectrometer detects the monomer, dimer, and trimer ions.

These expressions may be simplified via the substitutions

$$M = [A^+]_c, \quad D = (f_m/f_d)[A_2^+], \quad T = (f_m/f_t)[A_3^+] \quad (4)$$

$$d = (f_m \ell I) \sigma_d \rho_d \quad (5)$$

$$t = (f_m \ell I) \sigma_t \rho_t \quad (6)$$

to give

$$M = \alpha d + \beta t \quad (7)$$

$$D = \delta d + \epsilon t \quad (8)$$

$$T = \eta t \quad (9)$$

Note that the coefficients are so defined that

$$\alpha + \delta = 1 \quad (10)$$

$$\beta + \epsilon + \eta = 1 \quad (11)$$

Equations (5) and (6) define new quantities  $d$  and  $t$  proportional to the beam densities  $\rho_d$  and  $\rho_t$ , the common instrumental factors being collected inside the parentheses, because we are interested only in the functional shape of the dependence of the dimer and trimer beam densities on nozzle pressure. In other words, only the relative beam densities are needed. Equation (4) describes the correction of the observed ion intensities for the mass dependence of the detector efficiency, normalized to the efficiency for detecting monomer ions; corrections to the detector efficiency for ions born with high translational energies are neglected.

As a first step in the solution of Equations (7)-(11) we see that extrapolation of experimentally determined values of  $D/M$  to low nozzle pressures  $P$  such that  $t \ll d$  allows the determination of  $\delta/\alpha$  via

$$\lim_{P \rightarrow 0} (D/M) = (D/M)_0 = \delta/\alpha \quad (12)$$

Thus, from Equations (10) and (12)

$$\alpha = [1 + (D/M)_0]^{-1} \quad (13)$$

$$\delta = (D/M)_0 [1 + (D/M)_0]^{-1} \quad (14)$$

Data at a single additional pressure are insufficient to determine all seven unknown quantities (i.e.,  $d$  and  $t$  at that pressure plus the five coefficients) because there are only six equations. Data at two pressures are sufficient, however, since this provides nine equations to be solved for

nine unknowns, namely values of  $d$  and  $t$  at each pressure plus the five coefficients. Most of these equations are nonlinear with respect to the unknowns, so that attempts at a direct analytical solution only lead to intractable expressions. To circumvent this problem, the fact is exploited that normally  $d$  will maximize at some (unknown) nozzle pressure, so that for the value of  $d$  at some arbitrary pressure not too far above the maximum, a pressure below the maximum can be found for which  $d$  is the same, i.e., such that  $d_1 = d_2$  where subscript 1 means the lower pressure and subscript 2 means the higher. For such a pair of pressures it is easily shown from Equations (7)-(9) that

$$\delta/\alpha = (T_2 D_1 - T_1 D_2)/(T_2 M_1 - T_1 M_2) \quad (15)$$

Reasonable estimates of the nozzle pressure at which  $d$  is at its maximum will guide the choice of candidate pairs of pressures from which trial values of  $\delta/\alpha$  can be calculated from Equation (15) for comparison with the experimental value from Equation (12). Three pressure pairs should be chosen as close together as possible, but not too close because of the limited experimental accuracy. Once one or more pairs of pressures are found by trial-and-error for which  $\delta/\alpha$  from Equation (15) agrees with  $\delta/\alpha$  from Equation (12), the remaining three coefficients can be evaluated via the following expressions, where  $\Sigma = (M_2 - M_1) + (D_2 - D_1) + (T_2 - T_1)$ .

$$\beta = (M_2 - M_1)/\Sigma \quad (16)$$

$$\epsilon = (D_2 - D_1)/\Sigma \quad (17)$$

$$\eta = (T_2 - T_1)/\Sigma \quad (18)$$

Equations (16)-(18) are easily derived from Equations (7)-(9) and (11) for the condition  $d_1 = d_2$ .

With all five coefficients known, Equations (7) and (8) become two linear equations with two unknowns at any given nozzle pressure, so  $d$  and  $t$  can be evaluated point-by-point.

$$d = (\beta D - \epsilon M) / (\beta \delta - \alpha \epsilon) \quad (19)$$

$$t = (\delta M - \alpha D) / (\beta \delta - \alpha \epsilon) \quad (20)$$

Of course as the pressure rises until tetramers and larger clusters become important this method must fail. In practice such pressures are indicated by evaluation of Equation (9), where  $T$  becomes inaccurately predicted by  $\eta t$ , and by the behavior of  $d$ , which becomes unreasonably small or negative. It is to be expected that the latter inaccuracy will often cause the calculated nozzle pressure for maximum  $d$  to be somewhat too low. In extreme cases it could cause an apparent maximum where none exists.

We are now in a position to consider the problem of most interest to us, namely, product heterodimer optimization in expansions of binary mixtures. Let the mixture be comprised of gas A plus gas B, where A is the component of lower ionization potential. The dimer products of the expansion are then  $A_2$ , AB, and  $B_2$ , and the trimers are  $A_3$ ,  $A_2B$ ,  $AB_2$ , and  $B_3$ . The method described above is applied to this problem by generalization of  $M$ ,  $D$ , and  $T$ . Thus,  $M$  might be the sum of the intensities of monomer ions  $A^+$  and  $B^+$ , coming only from the dissociative ionization of clusters, and  $D$  might be the sum of the intensities of all dimer ions,  $A_2^+$ ,  $AB^+$  and  $B_2^+$ , where all of the component intensities are corrected for the mass dependence of the detector efficiency in analogy with Equation (4). The three most serious inaccuracies of this approximation are the following: (1) the maximum in  $d$  now refers to a composite maximum for all three dimers and will in general occur at a somewhat different pressure than the maximum of heterodimer AB alone; (2) the proportions of the various components in clusters of a given size will in general change with pressure, and this will make the coefficients  $\alpha$ ,  $\beta$ ,  $\delta$ ,  $\epsilon$ , and  $\eta$  somewhat pressure-dependent and therefore affect the calculated positions of the dimer maximum and the shapes of the  $d$  and  $t$  functions. In addition, the proportions of the

components, and therefore the values of the coefficients  $\alpha$ ,  $\beta$ ,  $\delta$ ,  $\epsilon$ , and  $\eta$ , will be dependent on the composition of the expanding gas; and (3) the maximum in d, being for a composite, will in general be more broad than it is for a single type of dimer, making it more difficult to locate and therefore the extracted coefficients correspondingly less certain. These problems can be partially eliminated under the following special conditions.

1. When the ionization potential of A is substantially smaller than that of B, the contribution to M of  $A^+$  from AB is much larger than the contribution of  $B^+$  from AB. Consequently, in the calculations of M, D, and T we omit the contributions from  $B^+$ ,  $B_2^+$ , and  $B_3^+$  in the respective summations, in the expectation that the fragment of highest ionization potential will always be negligible in the dissociative ionization of mixed clusters, e.g., that the production of  $B^+$  or  $B_2^+$  from  $AB_2$  will be very much less than the production of  $A^+$  or  $AB^+$ . In this way we effectively omit clusters  $B_2$  and  $B_3$  from d and t. The resulting redefinitions of M, D, and T are then, via generalization of Equation (4),

$$M = [A^+]_c \quad (21)$$

$$D = (f_A/f_{A_2})[A_2^+] + (f_A/f_{AB})[A \cdot B^+] \quad (22)$$

$$T = (f_A/f_{A_3})[A_3^+] + (f_A/f_{A_2B})[A_2B^+] + (f_A/f_{AB_2})[AB_2^+] \quad (23)$$

where  $[i^+]$  is the uncorrected intensity of the indicated ion  $i^+$ , the corresponding detection efficiency of which is given by  $f_i$ .

2. When the dissociation energies of the heterodimer and homodimer are greatly different, i.e., when  $D(A \cdot A) \ll D(A \cdot B)$  or  $D(A \cdot A) \gg D(A \cdot B)$ , the more strongly bound dimer will be formed and become optimum at much lower nozzle pressures than the more weakly bound dimer. Similar considerations apply to the trimers, so that if  $D(A \cdot A) \ll D(A \cdot B)$  and  $D(A_2 \cdot A) \ll D(A_2 \cdot B)$  the ion  $A_2^+$  comes essentially entirely from  $A_2B$  at the lowest nozzle pressures at which

it can be seen. Under such circumstances the omission of contributions from  $B^+$ ,  $B_2^+$ , and  $B_3^+$ , to M, D, and T will result in the optimization of the more strongly bound dimer almost exclusively. Thus, for example, in the expansion of an argon-benzene mixture, the calculation will find the nozzle pressure for the optimum beam density of  $(C_6H_6)_2$  with little or no admixture of  $C_6H_6 \cdot Ar$  because  $D((C_6H_6)_2) \gg D(C_6H_6 \cdot Ar)$ .

A crucial requirement of the method presented above is the availability of the quantity, M, which must be obtained by subtraction of the monomer ion intensity due only to the ionization of neutral monomers from the total monomer ion intensity. The procedure is described below. In electron impact or photon energy fragmentation, ions  $F^+$  of A are formed that require a substantial amount of energy beyond that needed just for the production of  $A^+$ , for example, the formation of  $C_4H_4^+$  from  $C_6H_6$ . We have observed that such high-energy fragments as  $F^+$  are not detectable from clusters  $A_n$ . Thus, the intensity ratio  $[A^+]/[F^+]$  can be measured under conditions where there are no clusters, e.g., at low nozzle pressure

$$\lim_{[A_n] \rightarrow 0} ([A^+]/[F^+]) = ([A^+]/[F^+])_0, n > 1 \quad (24)$$

and used to evaluate M at nozzle pressure P.

$$[A^+]_c = M = [A^+]_\rho - ([A^+]/[F^+])_0 [F^+]_\rho \quad (25)$$

Here, the square brackets mean the observed intensity of the ion that they enclose. Of course this procedure can only be applied to polyatomic gases.

However, there is a complication caused by the polyatomicity of A and B. In general, ions larger than  $A^+$  or  $B^+$  other than  $A_n^+$  or  $A_n B_m^+$  are formed. Usually this does not seriously interfere with the limited objective of locating the nozzle pressure for which the beam density of neutral dimers is at a maximum, but complicates the determination of the ratio d/t. To obtain d/t and to preserve the validity of Equations (10) and

(11), the intensities of the fragment ions must be included in the sums for M, D, and T. Consequently, we must further generalize the definitions of M, D, and T for this purpose. Equations (7) and (8), our original definitions of which confine M only to monomer ion and D only to dimer ions, also apply to the broadened definitions of M and D because both of these quantities include products of the ionization of the dimers plus contributions from trimers. We are then free to apportion the intensities of the dimer ion, its fragment monomer ion, and all of its other fragment ions to M or D in such a way as to facilitate the solution we seek. In general, inspection of the data will indicate that the intensities of some fragment ions rise more rapidly with increasing nozzle pressure than the intensities of others, because they are produced to a greater extent by the ionization of trimers (and larger clusters). Thus, in Equation (26) we may advantageously redefine M as the sum of the intensities of fragment ions  $M^+$  that rise relatively more slowly with increasing nozzle pressure, and D as the sum of the intensities of ions  $D^+$  that rise relatively more rapidly, where each term in the summations is appropriately corrected for detector efficiency. In practice, we have found that with this rule the fragment monomer ion intensity  $[A^+]_c$  is always included in M, the dimer ion intensities always go to D, and that it is usually straightforward to decide which term is more appropriate for each fragment ion intensity. Similarly, let T be the sum of the intensities of all ions  $T^+$  that can come from trimers or larger clusters excluding those that are required to come from clusters larger than trimers. This further generalization of M, D, and T, following the pattern of Equations (4) and (22) can be written

$$M = \sum_M (f_A/f_M) [M^+] \quad (26)$$

$$D = \sum_D (f_A/f_D) [D^+] \quad (27)$$

$$T = \sum_T (f_A/f_T) [T^+] \quad (28)$$

where, as before,  $f_i$  is the detector efficiency for ion  $i^+$ . Although in most systems that we have studied, the cluster ion spectra are dominated by species of the form  $A_n^+$ , or  $A_n B_m^+$ , where the fragments are unimportant, a few molecules, such as ammonia, provide conspicuous exceptions (Reference 20).

One sometimes wants to know the relative proportions of the neutral dimers and trimers in a molecular beam. It is useful to understand how well this information can be recovered from the values of  $d$  and  $t$  if the latter are obtained from the generalized definitions of  $D$  and  $T$  given above. The total ionization cross sections are contained in  $d$  and  $t$  as defined in Equations (5) and (6). It is reasonable to expect that at the high electron impact or photon energies at which the measurements are made the total ionization cross section of  $A_n$  is approximately proportional to  $n$ ; therefore,  $t$  should be multiplied by  $2/3$  for its proportion to  $d$  to be a reasonable estimate of the number density of neutral trimer clusters relative to dimer clusters, i.e., from Equations (5) and (6)

$$\rho_d/\rho_t = (\sigma_d/\sigma_t)t/d \approx (2/3)t/d \quad (29)$$

However, for mixed clusters one must not only use the relative total ionization cross sections of  $A$  and  $B$ , but also know the relative proportions of the different dimer and trimer species in the beam. Since the relative proportions are not forthcoming from this method, estimates of the proportion of mixed dimers to trimers must remain rather uncertain. As a rough rule of thumb we compare  $(2/3)t$  with  $d$  for mixed clusters, but recognize that the true relationship can deviate considerably from this rule.

i

In summary, it should be emphasized that the above-described method of locating the nozzle pressure that maximizes the beam density of neutral weak dimers is only approximate. However, it serves as a guide for selection of conditions for the easiest possible observations of the dimers consistent with minimal interference from larger clusters. This purpose demands only

modest accuracy. Probably the most serious source of inaccuracy for pure gases is the truncation of the calculation at the trimers, while for mixed gases the method suffers in addition from our neglect to consider separately all of the different molecular combinations involved for each size cluster. In particular, it is to be expected that often the dimer maximum will occur at a somewhat higher nozzle pressure than is indicated by this method, because the trimer is increasingly overestimated with increasing pressure, causing the dimer to be underestimated. Fortunately, both inaccuracies are such that any error in choosing the optimum experimental conditions for dimers will cause an overestimate of the possible interference from trimers. The prescription has proven more than adequate for the limited purpose for which it is intended and is sufficiently straightforward that it can be applied while the data are being taken. Most immediately, we find the optimum nozzle conditions by matching  $\delta/\alpha$  from Equation (15) with  $\delta/\alpha$  from Equation (12). Furthermore, it is necessary to make ancillary measurements around this pressure to see whether a lower pressure must be used to avoid interference from trimers. In other words, the five coefficients and  $d$  and  $t$  themselves need never be explicitly evaluated. In fact, it is easily shown that the shape of the  $d$  function is independent of the mass dependence of the detector efficiency, so that this correction can be neglected if the position of the maximum is the only information sought.

## SECTION III

### RESULTS

To provide a context for understanding the experimental results, three systems were studied: (a) a fuel ( $C_6H_6$ ) plus  $O_2$ ; (b) a mild extinguishant ( $C_6F_6$ ) plus  $O_2$ ; and (c) Halon 1301 ( $CF_3Br$ ) plus  $O_2$ . Weakly bound molecular complexes of all of these pairs were produced in supersonic nozzle expansions, and their dissociation energies were determined. The results are given in Table 1. The dissociation energies are all small, 2 kcal mol<sup>-1</sup> or less, confirming the weak binding. In the case of  $CF_3Br$ , the complex with oxygen could be formed in low concentration, but the homoclusters,  $(CFBr)_n$ ,  $n > 1$ , were present in surprising abundance. Interference from these clusters was minimized by working in very dilute mixtures (195:5) of  $CF_3Br$  in  $O_2$  and maintaining low nozzle stagnation pressures.

In both  $C_6H_6 \cdot O_2$  and  $C_6F_6 \cdot O_2$  cases, oxygenated fragments ( $C_6H_6O^+$  and  $C_6F_6O^+$ ) could be readily observed with the mass spectrometer. An attempt was made to prepare oxygenated fragments of  $CF_3Br \cdot O_2$  by dissociative photoionization. Figure 3 gives the mass spectrum of neat  $CF_3Br$  as seen in a molecular beam with a nozzle pressure of 97 torr. The fragmentation pattern is straightforward with very little parent ion  $CF_3Br^+$  appearing at  $m/e = 148, 150$  and fragments as follows:  $CF_2Br^+$  ( $m/e = 129, 131$ );  $Br^+$  ( $m/e = 79, 81$ );  $CF_3^+$  ( $m/e = 69$ ); and  $CF_2^+$  ( $m/e = 50$ ). The dominant peak is due to  $CF_3^+$ . Care must be taken in comparing intensities of the peaks, however, because the transmission efficiency of the quadrupole is a strong function of mass number. The inset displays on an expanded scale the  $m/e = 160 - 230$  portion of the mass spectrum to show the low background in this mass range. In particular, there is some signal in the vicinity of  $m/e = 166 - 171$ , but virtually none at  $m/e = 180, 182$ .

TABLE 1. DISSOCIATION ENERGIES OF THE WEAK MOLECULAR COMPLEXES  
 $C_6H_6 \cdot O_2$ ,  $C_6F_6 \cdot O_2$ ,  $CF_3Br \cdot O_2$ , AND THEIR IONS.

Mixture	Composition	Species	$D^0_o$ , kcal/mol <sup>-1</sup>	$D^0_{298}$ , kcal/mol <sup>-1</sup>
$C_6H_6 + O_2$	0.3:99.7	$C_6H_6 \cdot O_2$	$1.20 \pm 0.45$	$0.5 \pm 0.5$
		$C_6H_6 \cdot O_2^+$	$2.86 \pm 0.48$	
$C_6F_6 + O_2$	0.3:99.7	$C_6F_6 \cdot O_2$	$2.2 \pm 0.5$	
		$C_6F_6 \cdot O_2^+$	<sup>a</sup> 3.3	
$CF_3Br + O_2$	5:95	$CF_3Br \cdot O_2$	< <sup>a</sup> 2	
		$CF_3Br \cdot O_2^+$	> <sup>a</sup> 3	

<sup>a</sup>Unrefined results.

The weak complex  $CF_3Br \cdot O_2$  was prepared by expanding a 1:20 mixture of  $CF_3Br$  in  $O_2$  through the nozzle at a pressure of 1741 torr and cooling the nozzle to 1 °C. The mass spectrum obtained using 700 Å light is shown in Figure 4. Only the higher mass region,  $m/e = 110-250$ , is shown in this figure. Note the two sets of peaks due to ionization of the monomer  $CF_3Br$  at  $m/e = 148, 150$  ( $CF_3Br^+$ ) and  $m/e = 129, 131$  ( $CF_2Br^+$ ). The inset gives the expanded scale mass spectrum where species containing two bromine atoms can be seen above the background (cf. Figure 3) at  $m/e = 180, 182$  and at  $m/e = 217, 219$ . These are identified as  $CF_3Br \cdot O_2^+$  and  $(CF_3)_2Br^+$ , respectively. The latter fragment comes from a  $(CF_3Br)_2$  or larger cluster, which forms in

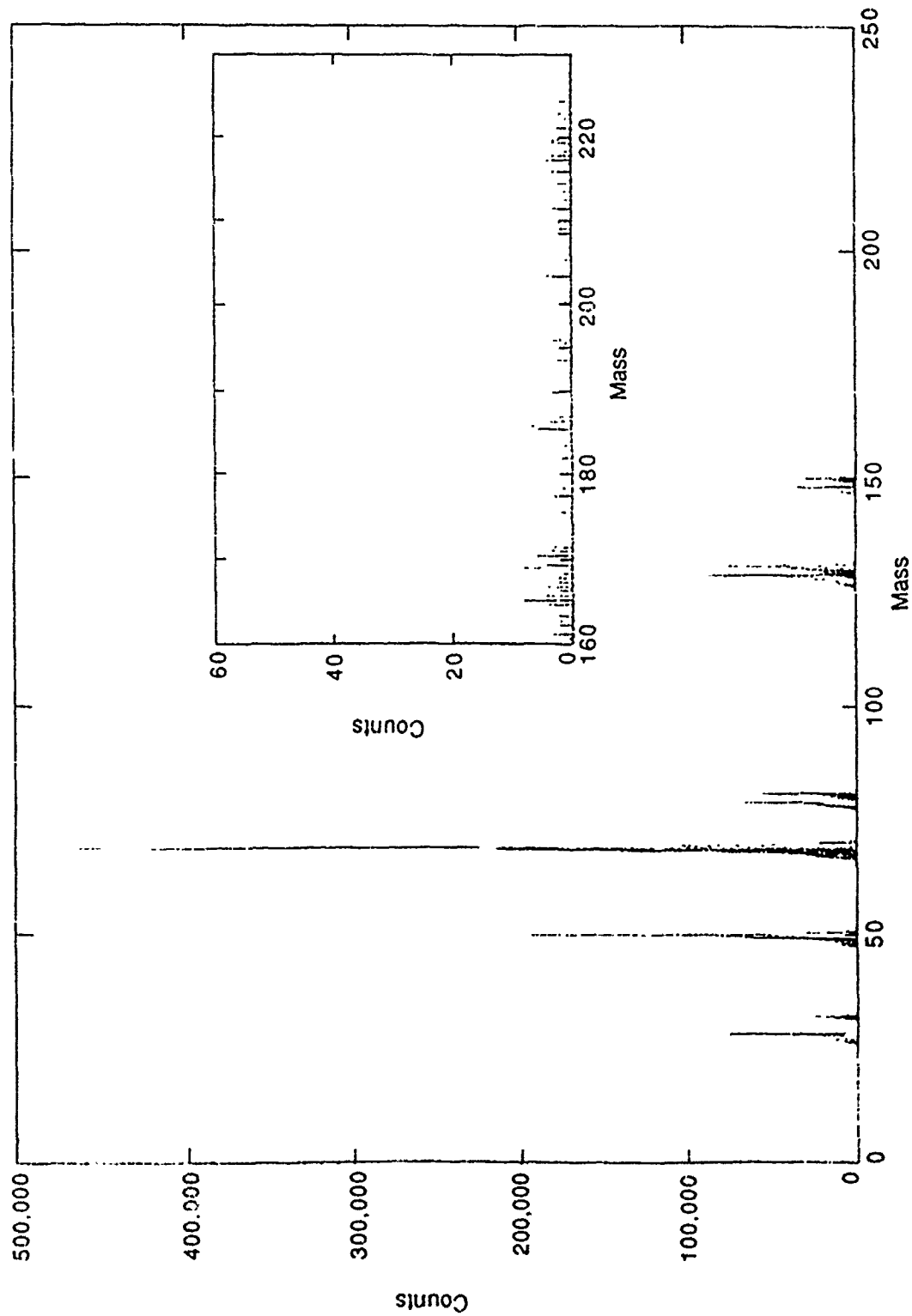


Figure 3. Mass Spectrum of  $\text{CF}_3\text{Br}$  at  $584 \text{ \AA}$  (21.22 eV) with a Nozzle Pressure of 97 torr. The inset shows an expanded scale of the  $m/e = 160-230$  region.

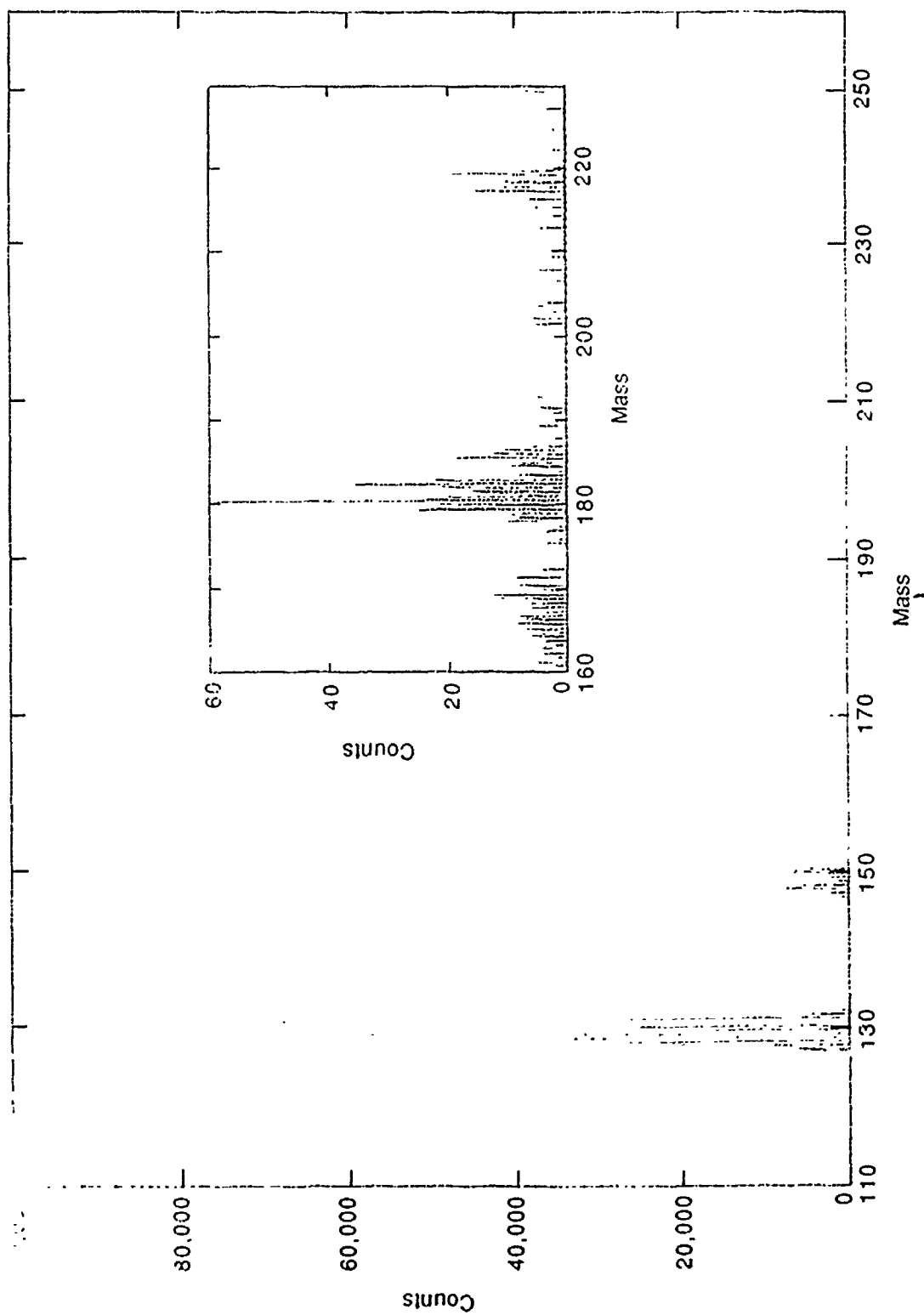


Figure 4 Mass Spectrum of a 1:20 Mixture of  $\text{CF}_3\text{Br}$  in  $\text{O}_2$  at 700 Å. The nozzle stagnation pressure was 1741 torr and the mass range displayed is  $m/e = 110\text{-}250$ . The inset gives the expanded scale portion over the mass range of  $m/e = 160\text{-}230$ .

appreciable abundance even in this dilute mixture. Although the amount of  $\text{CF}_3\text{Br}\cdot\text{O}_2$  is small, the signal is sufficient to determine the ionization potential of the complex.

Photoion yield curves through the ionization threshold region were run for both  $\text{CF}_3\text{Br}$  and  $\text{CF}_3\text{Br}\cdot\text{O}_2$  (Figures 5-7). The curve in Figure 5 has been analyzed to give an ionization threshold of  $\text{CF}_3\text{Br}$  at 1078 Å, which corresponds to an ionization potential of 11.50 eV. The dissociation energy of the  $\text{F}_3\text{C}-\text{Br}$  bond is known to be 3.78 eV = 87.2 kcal mol<sup>-1</sup>. This value is typical of carbon-bromine bond strengths in organic molecules.

The photoion yield curves in Figures 6 and 7 have been analyzed to give an ionization potential for the formation of  $\text{CF}_3\text{Br}\cdot\text{O}_2^+$  from  $\text{CF}_3\text{Br}\cdot\text{O}_2$  of 1033 Å = 11.45 eV. The decrease in ionization potential is typical of many observations of cluster formation; however, it is much smaller than customarily noticed. It is not uncommon to observe ionization potential decreases of 0.5 - 0.7 eV in contrast to the change of 0.05 eV seen here. This dramatic observation suggests unusual bonding properties in the  $\text{CF}_3\text{Br}\cdot\text{O}_2^+$  cation. Combining the ionization potentials of  $\text{CF}_3\text{Br}$  and  $\text{CF}_3\text{Br}\cdot\text{O}_2$  with the measured dissociation energy of the weak complex  $\text{CF}_3\text{Br}\cdot\text{O}_2$ , we estimate a bond dissociation energy,  $\text{CF}_3^+\text{Br}\cdot\text{O}_2$ , in the ion of approximately 3 kcal mol<sup>-1</sup> (Table 1). This bond strength is very similar to cation bond strengths in  $\text{C}_6\text{H}_6\cdot\text{O}_2$  and  $\text{C}_6\text{F}_6\cdot\text{O}_2^+$ . The result suggests that one or more of the bonds in  $\text{CF}_3\text{Br}^+$  are unusual. Therefore, the appearance potential of  $\text{CF}_3^+$  from  $\text{CF}_3\text{Br}$  was measured by dissociative photoionization of a molecular beam of  $\text{CF}_3\text{Br} + \text{O}_2$ . The results are shown in Figure 8.

By applying second order corrections to the curve in Figure 8, an appearance potential of 1033 Å = 12.0 eV for  $\text{CF}_3^+$  from  $\text{CF}_3\text{Br}$  has been determined. This result can be combined with the ionization potential of  $\text{CF}_3\text{Br}$  (11.50 eV) to give a bond strength of the  $\text{C}-\text{Br}$  bond in  $\text{F}_3\text{C}^+-\text{Br}$  of 0.5 kcal mol<sup>-1</sup>. This is an extremely weak bond and can not involve a normal bond in the sense of electron sharing between  $\text{CF}_3^+$  and Br.

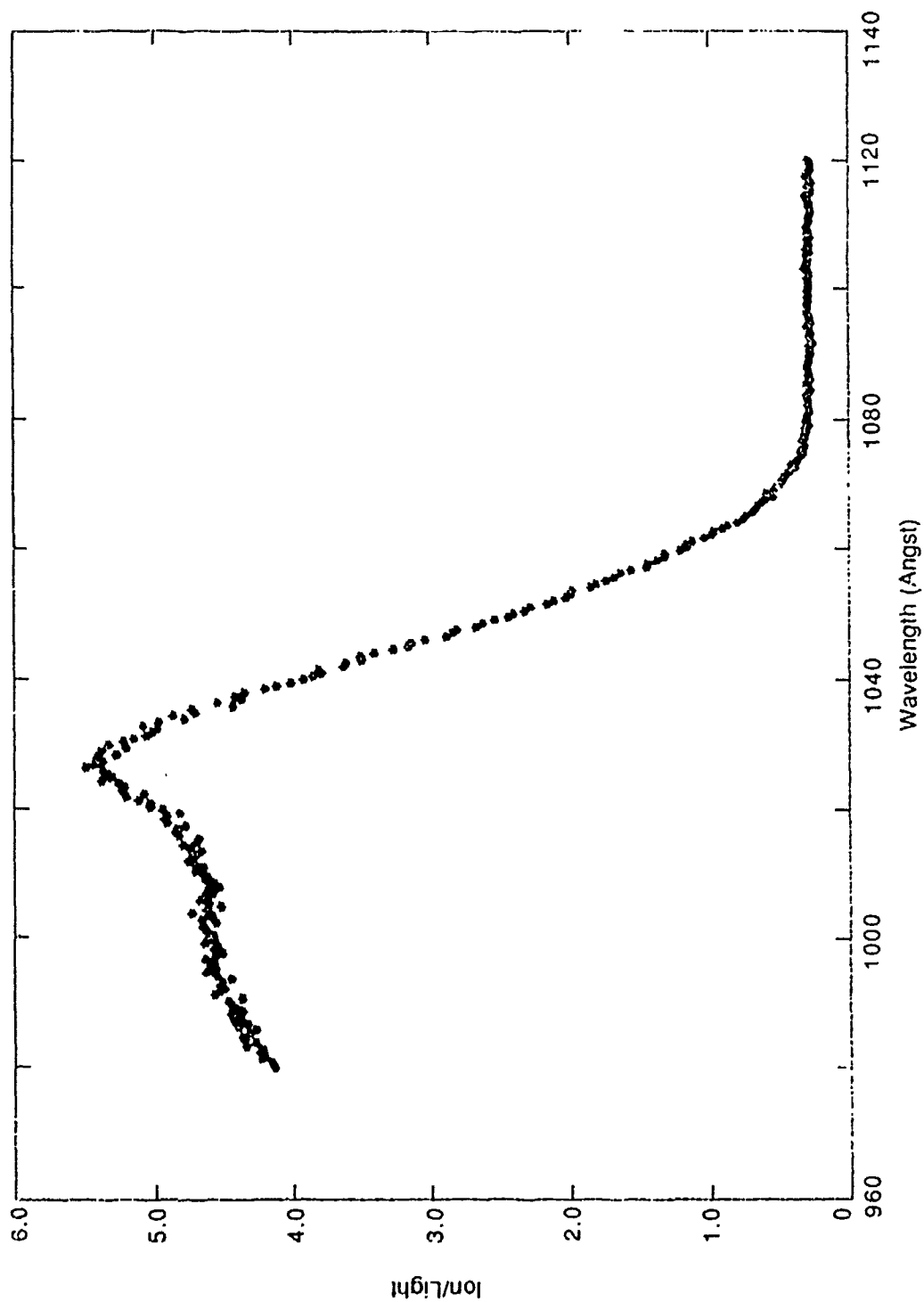


Figure 5.  $\text{CF}_3\text{Br}^+$  Wavescan, Range 980-1120 Å. Observed intensities of the ion  $\text{CF}_3\text{Br}^+$  produced by direct ionization of neat  $\text{CF}_3\text{Br}$  at 499 torr nozzle pressure in 0.5 Å intervals. No LiF filter was used and corrections for second-order contributions have not been applied

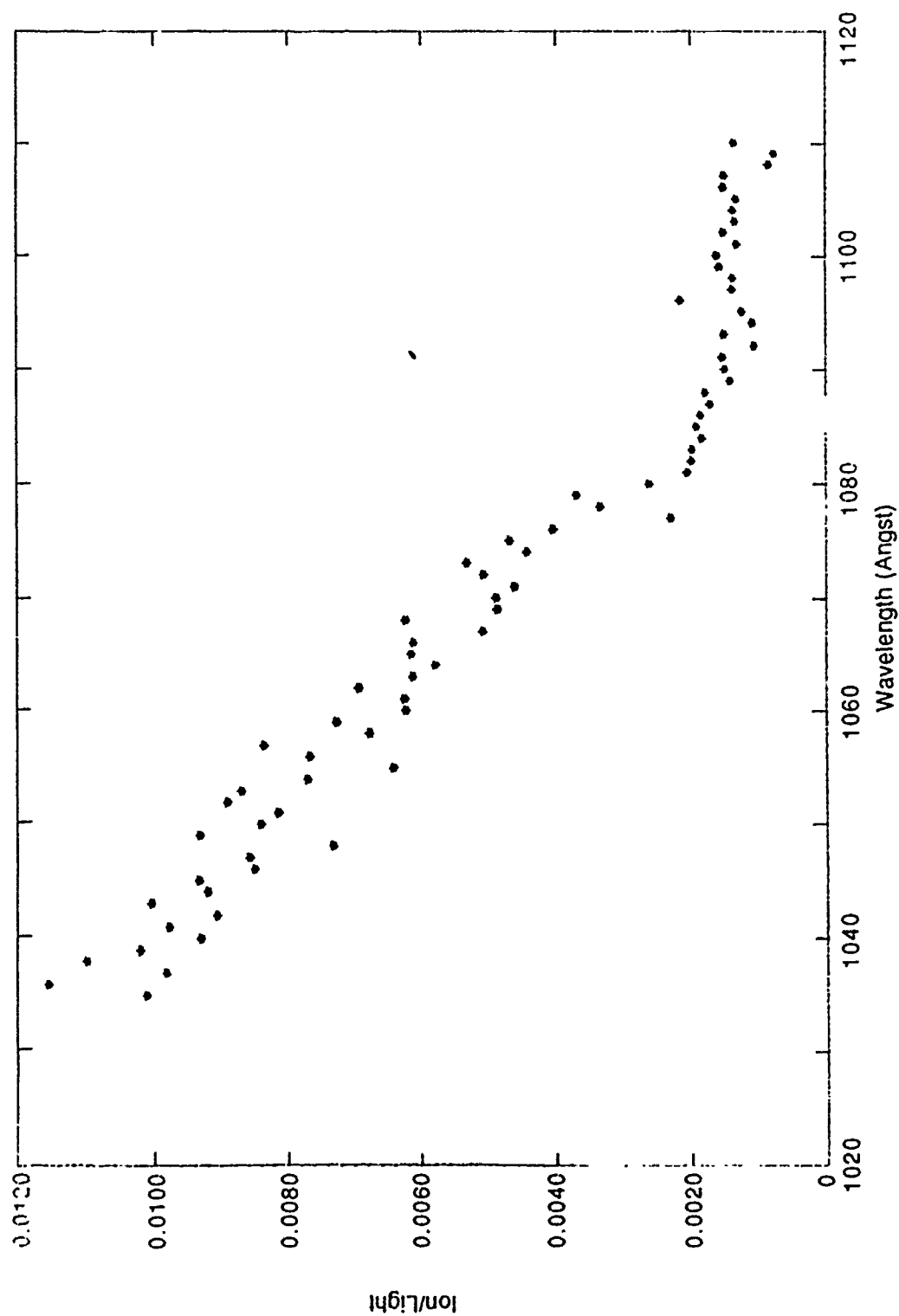


Figure 6.  $\text{CF}_3\text{BrO}_2^+$  Wavescan, Range 1035-1110 Å. Threshold photoion yield curves for the production of  $\text{CF}_3\text{BrO}_2^+$  from  $\text{CF}_3\text{Br-O}_2$  with a nozzle pressure of 1:20  $\text{CF}_3\text{Br} + \text{O}_2$  at 1750 torr and with no LiF window. Second-order corrections have not been applied. The intervals were 1 Å, and the total counting time at each wavelength was 70 sec.

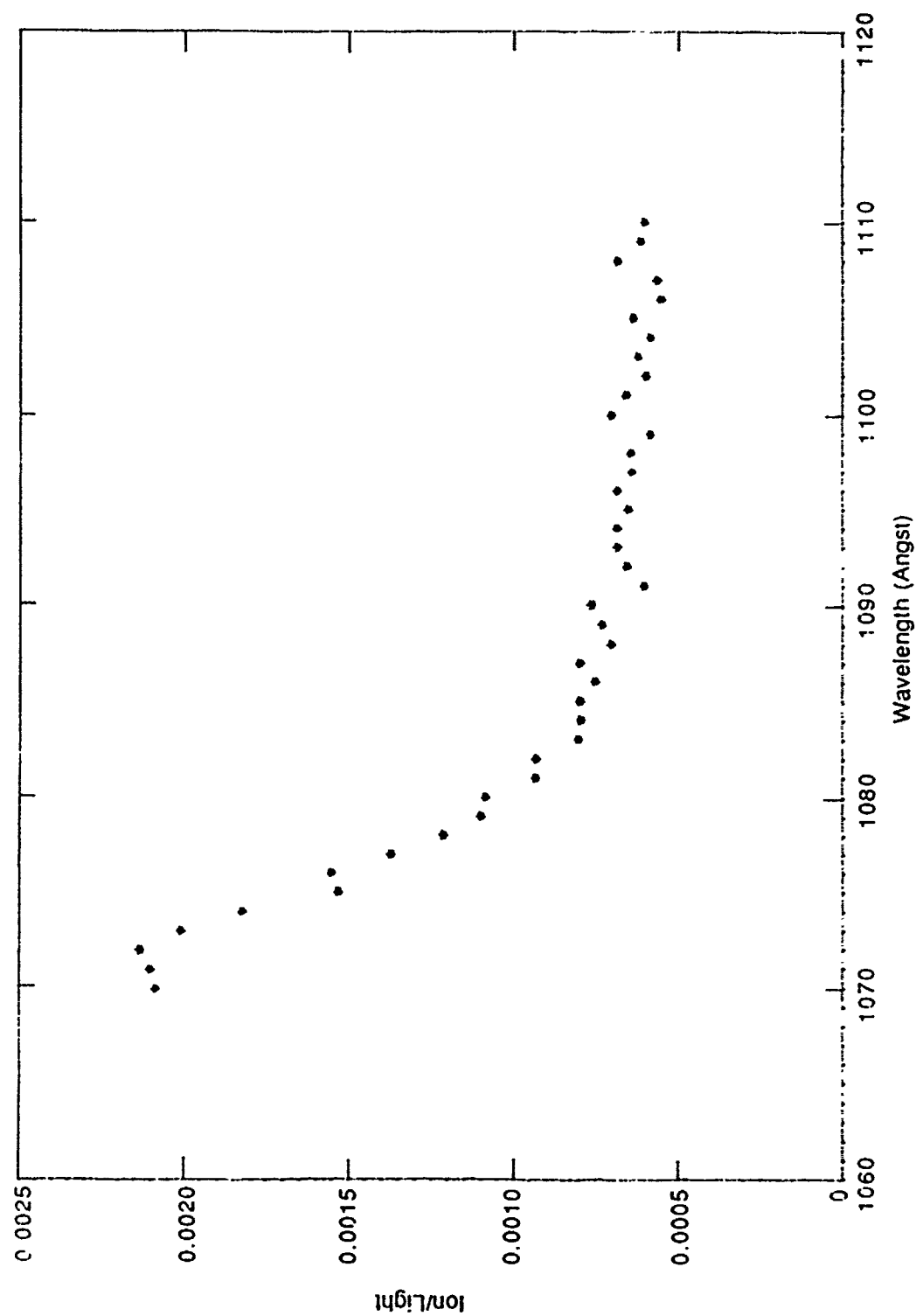


Figure 7.  $\text{CF}_3\text{BrO}_2^+$  Wavescan, Range 1070-1110 Å. Threshold photoion yield curves for the production of  $\text{CF}_3\text{BrO}_2^+$  from  $\text{CF}_3\text{Br} + \text{O}_2$  with a nozzle pressure of 1:20  $\text{CF}_3\text{Br} + \text{O}_2$  at 1750 torr and with no LiF window. Second-order corrections have not been applied. The intervals were 1 Å, with a total counting time of 280 sec per point.

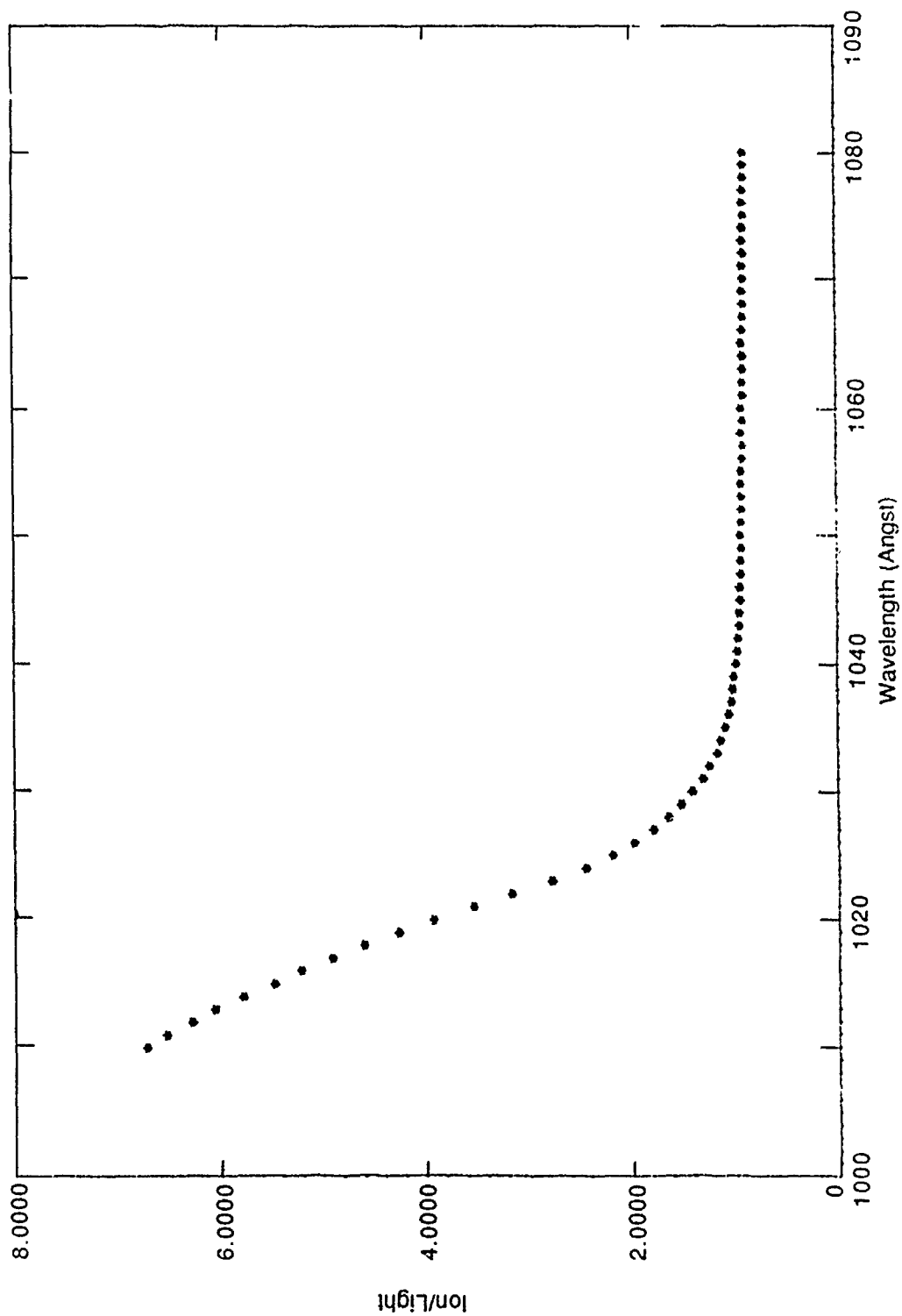


Figure 8.  $\text{CF}_3^+$  Wavescan, Range 1010-1080 Å. Observed intensities of the ion  $\text{CF}_3^+$  produced by direct ionization of  $\text{CF}_3\text{Br}$  in a 1:20 mixture of  $\text{CF}_3\text{Br} + \text{O}_2$  at 604 torr nozzle pressure in 1 Å intervals. No LiF filter was used. The nozzle temperature was 1.1° C.

It is characteristic of an ion-induced dipole interaction between these species. It appears that this weak bond is the basis for the very small shift in ionization potential in  $\text{CF}_3\text{Br}\cdot\text{O}_2$ .

The thermodynamic information for the species in the  $\text{CF}_3\text{Br}$  system is collected in the energy diagram shown in Figure 9.

A careful and detailed search of the mass spectrum for oxygenated fragments of  $\text{CF}_3\text{Br}\cdot\text{O}_2$  prepared by dissociative photoionization was conducted. It was discussed earlier that oxygenated fragments were observed in the  $\text{C}_6\text{H}_6\cdot\text{O}_2$  and  $\text{C}_6\text{F}_6\cdot\text{O}_2$  systems. Figure 10 shows the mass spectra for the regions in which  $\text{CF}_3\text{O}^+$  ( $m/e = 85$ ),  $\text{CF}_2\text{BrO}^+$  ( $m/e = 145, 147$ ), and  $\text{CF}_3\text{BrO}^+$  ( $m/e = 164, 166$ ) would be expected to appear. As can be seen, no distinct peaks can be observed in the  $m/e = 83-87$  or  $143-149$  regions. The signal here is background only. Note that the characteristic set of two peaks due to the bromine isotopes is completely absent in the  $m/e = 143-149$  segment. The situation is somewhat less clear at  $m/e = 145, 147$  because this region is located in the low mass wing of the  $\text{CF}_3\text{Br}^+$  parent ion at  $m/e = 148, 150$ . Nevertheless, no feature resembling the doublet expected for the two bromine isotopes appears at the appropriate masses. Although this study was repeated several times at different compositions and nozzle pressures, no oxygenated fragments of  $\text{CF}_3\text{Br}\cdot\text{O}_2$  dissociative photoionization were detected.

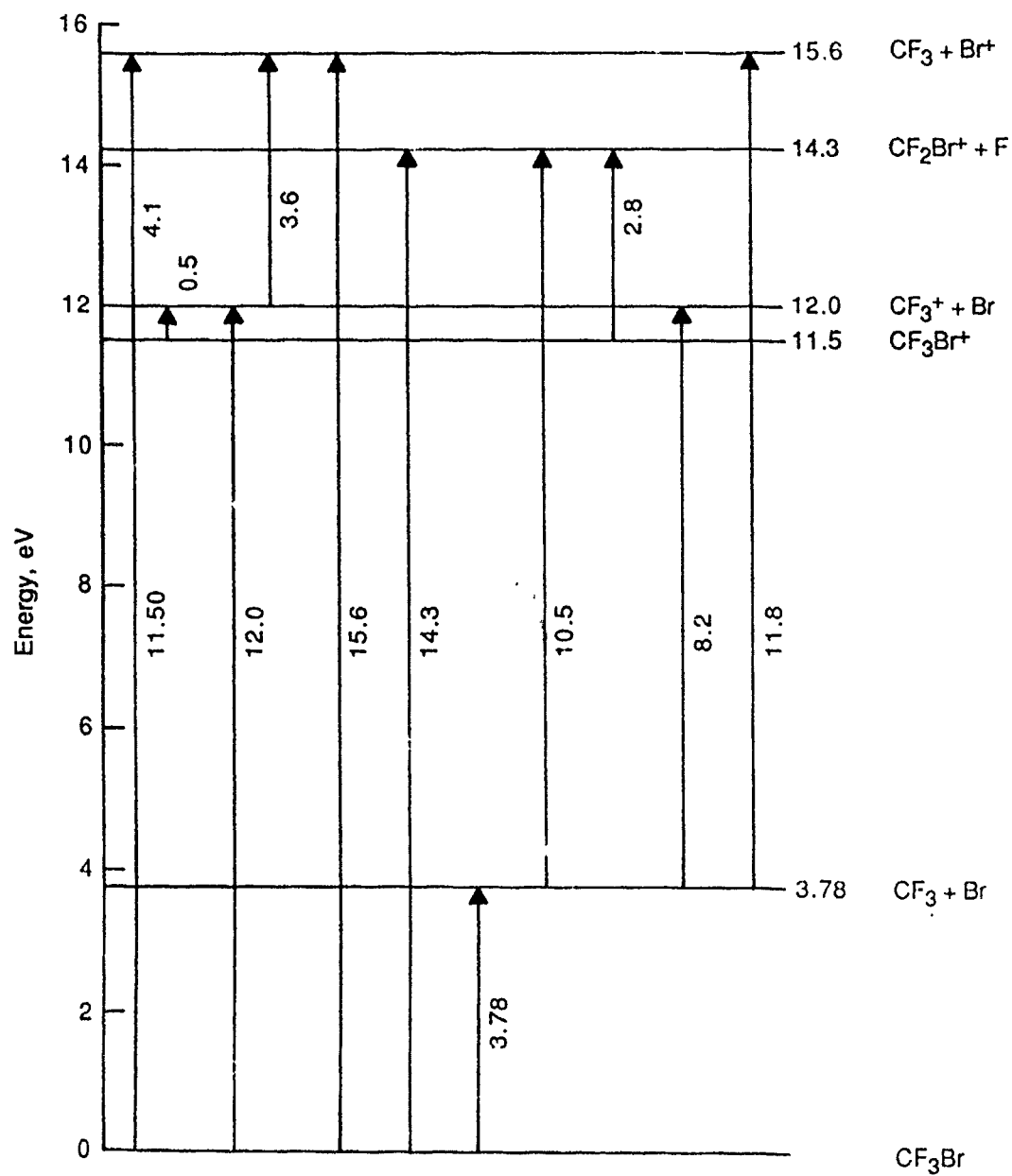


Figure 9. Energy Diagram for the Neutral and Ionic Species in the CF<sub>3</sub>Br System.

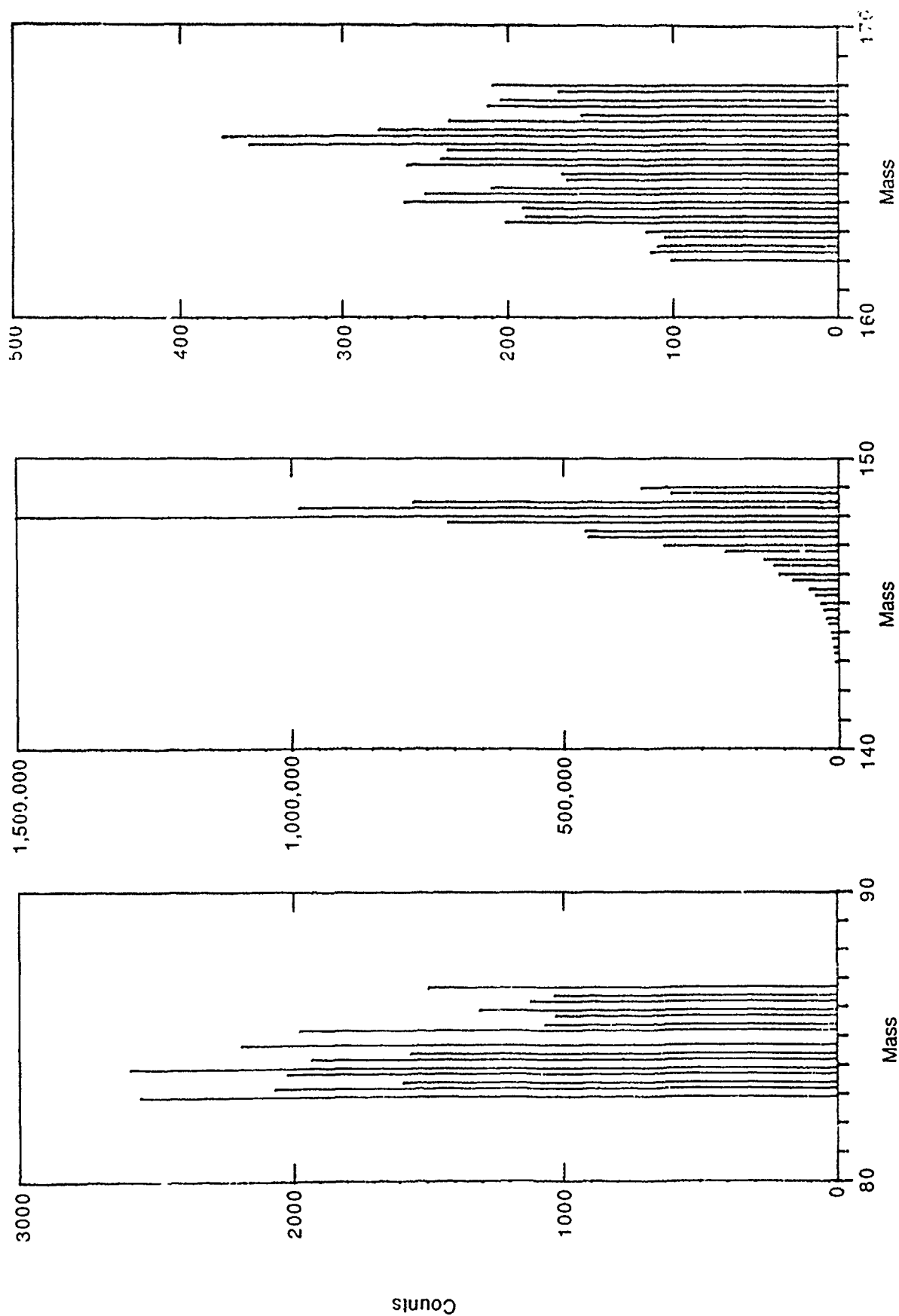


Figure 10. More Detailed Mass Spectra of 1:20  $\text{CF}_3\text{Br}:\text{O}_2$  at 700 Å with a Nozzle Pressure of 1750 torr. The ranges covered are  $m/e$  - 83-87, 143-149, and 162-168 in 0.25 amu steps. The counting time at each mass setting was 40 sec.

## SECTION IV

### CONCLUSIONS

The weakly bound molecular complex between Halon 1301 ( $\text{CF}_3\text{Br}$ ) and  $\text{O}_2$  has been studied by photoionization mass spectrometry in a molecular beam. Ionization and appearance potentials for many of the species in this binary system have been determined. The most striking result is the inability to detect oxygenated fragments of dissociative photoionization of the complex  $\text{CF}_3\text{Br}\cdot\text{O}_2$ . This is doubtless because of the fragility of  $\text{CF}_3\text{Br}^+$ , for which the  $\text{CF}_3^+-\text{Br}$  bond strength was measured to be only  $12 \text{ kcal mol}^{-1}$ . These results are so extraordinary that they yield a number of implications for the role of  $\text{CF}_3\text{Br}$  in fire extinguishment.

1. A reevaluation of the canonical mechanism for interaction of  $\text{CF}_3\text{Br}$  with flame free radicals may be necessary. The results suggest that  $\text{CF}_3\text{Br}$  may not serve as a trap for the O-atoms in a flame. Perhaps a supplementary oxygen atom trapping agent could be found to enhance the fire extinguishment properties of a halon or halon replacement.
2. The extremely weak C-Br bond in  $\text{CF}_3\text{Br}^+$  suggests that Br atoms enter the flame via the ion  $\text{CF}_3\text{Br}^+$  and not from  $\text{CF}_3\text{Br}$  itself. If this is substantiated, the door to many possible alternate agents is opened.
3. The role of the  $\text{CF}_3$  portion of the halon may be more significant than previously suspected. It may not simply be a spectator in the process of free radical trapping agent release but a critically active participant.
4. If Br does serve the role of a flame free radical trapping agent, the radical trapped must be H or OH. The evidence presented here shows that Br does not react well with O.

## SECTION V

### RECOMMENDATIONS FOR FUTURE WORK

The results of this study focused attention on the interaction between Halon 1301 ( $\text{CF}_3\text{Br}$ ) and the flame free radical O as generated from the stable diatomic precursor,  $\text{O}_2$ . Very significant results were obtained. Future work should direct attention to the two other members of the triad of flame free radicals, H and OH. Some further work with an alternative source of O may prove useful. Therefore, it is recommended that the dissociative photoionization approach to weakly bound clusters of Halon 1301 and flame free radical precursors be extended to H and OH precursors. Likely candidates for study are HCl or HBr as H atom precursors and  $\text{H}_2\text{O}$  as an OH radical precursor. An alternate source of O atoms is  $\text{NO}_2$ . The complex of  $\text{NO}_2$  with  $\text{CF}_3\text{Br}$  should also be studied.

These results should provide a reasonably good picture of the early chemistry of halon-flame interaction and therefore may be expected to give a solid basis for suggesting alternate agents.

## REFERENCES

1. Lu, C. S., and Carr, H. E., Review of Scientific Instruments, Vol. 33, p. 823, 1962.
  2. Giese, C. F., Review of Scientific Instruments, Vol. 30, p. 260, 1959.
  3. Herzberg, G., and Howe, L. L., Canadian Journal of Physics, Vol. 37, p. 636, 1959.
  4. Samson, J. A. R., Techniques of Vacuum Ultraviolet Spectroscopy, Wiley, New York, 1967, p. 139.
  5. White, M. G., and Grover, J. R. Chemical Physics, Vol. 79, pp. 4124-4131, 1983.
  6. Masuoka, T., and Samson, J. A. R., Journal de Chimie Physique, Vol. 77, pp. 623-630, 1980.
  7. Hitchcock, A. P., and Van der Wiel, M. J., Journal Physical Chemistry, Vol. 89, pp. 2153-2169, 1979.
  8. Grover, J. R., and Walters, E. A., Journal of Physical Chemistry, Vol. 90, p. 620, 1986.
  9. Levy, D. H., Annual Review of Physical Chemistry, Vol. 31, pp. 197-215, 1980.
  10. Balle, T. J., and Flygare, W. H., Review of Scientific Instruments, Vol. 52, pp. 33-45, 1981.
  11. Buck, U., and Meyer, H., Physics Review Letters, Vol. 52., pp. 109-112, 1984.
  12. Jonkman, H. T., Even, U., and Kommandeur, J., Journal of Physical Chemistry, Vol. 89, pp. 4240-4243, 1985.
  13. Lee, N., and Fenn, J. B., Review of Scientific Instruments, Vol. 49, pp. 1269-1272, 1978.
  14. Fenn, J. B., and Lee, N., Review of Scientific Instruments, Vol. 53, pp. 1494-1495, 1982.
- Gentry, W. R., Review of Scientific Instruments, Vol. 53, pp. 1492-1493, 1982.

16. Van Deursen, A., and Reuss, J., International Journal of Mass Spectrometry and Ion Physics, Vol. 23, pp 109-122, 1977.
17. Walters, E. A., Grover, J. R., Newman, J. K., and White, M. G., Chemical Physics Letters, Vol. III, pp. 190-194, 1984.
18. Walters, E. A., Grover, J. R., White, M. G., and Hui, E. T., Journal of Physical Chemistry, Vol. 89, pp. 3814-3818, 1985.
19. Grover, J. R., Walters, E. A., Newman, J. K., and White, M. G., Journal of the American Chemical Society, Vol. 107, pp. 7329-7339, 1985.
20. Ceyer, S. T., Tiedemann, P. W., Mahan, B. H., and Lee, Y. T., Journal of Chemical Physics, Vol. 70, pp. 14-17, 1979.